Nucleosynthesis of light nuclei and hypernuclei in central Au+Au collisions at $\sqrt{s_{NN}}$=3 GeV

N. Buyukcizmeci[1], T. Reichert[2,3,4], A.S. Botvina[2,3], M. Bleicher[2,3,5]

[1]*Department of Physics, Selçuk University, 42079 Kampüs, Konya, Türkiye*
[2]*Institut für Theoretische Physik, J.W. Goethe University, D-60438 Frankfurt am Main, Germany*
[3] *Helmholtz Research Academy Hesse for FAIR (HFHF), GSI Helmholtz Center,*
Campus Frankfurt, Max-von-Laue-Str. 12, 60438 Frankfurt am Main, Germany
[4] *Frankfurt Institute for Advanced Studies (FIAS),*
Ruth-Moufang-Str.1, D-60438 Frankfurt am Main, Germany and
[5]*GSI Helmholtz Center for Heavy Ion Research, Planckstr.1, Darmstadt, Germany*

We analyze the experimental data on nuclei and hypernuclei yields recently obtained by the STAR collaboration. The hybrid dynamical and statistical approaches which have been developed previously are able to describe the experimental data reasonably. We discuss the intriguing difference between the yields of normal nuclei and hypernuclei which may be related to the properties of hypermatter at subnuclear densities. New (hyper-)nuclei could be detected via particle correlations. Such measurements are important to pin down the production mechanism.

I. INTRODUCTION

During recent years the production of new nuclei has become again one of the central topics in relativistic nuclear reaction studies. It is known since the late 1970s that many different light complex nuclei can be formed in central nucleus-nucleus collisions [1]. Later on these studies were considerably extended and presently they involve the production of both normal nuclei and hypernuclei, including exotic nuclear species. In central relativistic nucleus-nucleus collisions the yields and spectra of hydrogen and helium isotopes have been observed. In addition, more heavy species, like Li, Be and others were also under examination [2–5]. It is commonly accepted these light nuclei are mostly formed on later stages of the reaction from nucleons which are primary produced. Although other production mechanisms, like direct thermal production, have been proposed [6]. This indicates that nucleosynthesis mechanisms can be studied in these processes and they may complement and lead to better understanding the nucleosynthesis in the Universe. Recently the detection of hypernuclei was also reported in relativistic nuclear collisions [7–10] providing an opportunity to extend the nucleosynthesis investigation to strange nuclear matter. Also heavy-ion collisions open new possibilities to obtain novel hypernuclei, including multi-strange and exotic hypernuclei, which are more difficult to produce in other reactions.

In this paper we further develop the theory of hypernuclei production by analyzing the formation of light nuclei and hypernuclei which were measured at the STAR experiments with fixed targets in gold+gold collisions [9]. As we have previously demonstrated in our calculations the reactions with a beam energy around 3–10 GeV per nucleon lead to a large production of hyperons and can provide essential yields of hypernuclei [11, 12]. Therefore, the systematic comparison with experiments in this en-

ergy range is important for both central and peripheral collisions. Recently we have succeeded to describe the formation of complex normal nuclei in central collisions [13, 14]. Now we demonstrate that the same nucleosynthesis mechanism can be effectively applied to describe the hypernuclear production too.

II. MECHANISMS OF THE NUCLEI PRODUCTION

In the most general consideration the reaction may be subdivided into several stages: (1) The dynamical stage which can lead to the formation of an equilibrated nuclear system. (2) The statistical fragmentation of such system into individual fragments, which can be accompanied by the de-excitation of these hot fragments if they are in an excited state. Various transport models are currently used for the description of the dynamical stage of the nuclear reaction at high energies. They take into account the hadron-hadron interactions including the secondary interactions and the decay of hadron resonances (e.g. [15, 16]). For this reason they preserve important correlations between hadrons originating from the primary interactions in each event, which are ignored when we consider the final inclusive particle spectra only. Using dynamical models it was established that many particles are involved in these processes by the intensive rescattering leading to collective behaviour during the evolution at the collisions. In peripheral collisions the produced high energy particles leave the system and the remaining nucleons form an excited system (a residue). We may expect that this system evolves toward a state which is mostly determined by the statistical properties of the excited nuclear matter. Its decay leads to the production of various new nuclei (see, e.g., [17–19]).

It is typical for relativistic collisions of two nuclei that

as a result of the dynamical production of individual baryons a substantial amount of hyperons and nucleons populate the midrapidity kinematic region. In this region new nuclei can be formed from these particles via their subsequent interaction in the diluted nuclear matter during the expansion process. Generally, at the end of the dynamical stage (at a time around ∼20-40 fm/c after the beginning of the collision) many new-born baryons escape from the colliding nuclei remnants. Some of these baryons may be located in the vicinity of each other with local subnuclear densities around ∼$0.1\rho_0$ ($\rho_0 \approx 0.15 \, \text{fm}^{-3}$ being the ground state nuclear density). This nuclear matter density corresponds to the coexistence region in the nuclear liquid-gas type phase transition. It is the proper place of the synthesis of new nuclei, because the remaining attraction between baryons can lead to complex fragment formation. We expect that such nucleation processes will mostly produce the light nuclei. The formation process may be simulated as the baryon attraction using potentials within the dynamical transport models [20–22], or within phenomenological coalescence models [3, 23–26]. However, as we have demonstrated recently [13, 14], the clusterization processes can be reasonably described as the statistical formation of nuclei in the low density matter in local chemical equilibrium.

To describe the dynamical reaction part we use the transport UrQMD model [16, 27], which is modified for the present studies. UrQMD is quite successful in the description of a large body of experimental data on particle production [28, 29]. The current version of UrQMD include up to 70 baryonic species (including their antiparticles), as well as up to 40 different mesonic species, which participate in binary interactions. In the present calculations the hard Skyrme type equation of state is used which includes also for the attraction between baryons. We explicitly conserve the net-baryon number, net-electric-charge, and net-strangeness as well as the total energy and momentum. The produced particles can be located at various rapidities, however, the main part is concentrated in the midrapidity region. After a time of 20–40 fm/c the strong interactions leading to the new particle formation cease and the system start to decouple. Such kind of a freeze-out is a general feature captures in the transport approaches [30]. In that time-moment we consider the relative coordinate positions and velocities of the produced baryons. We select the nuclear clusters according to the coordinates and velocities proximity, as was suggested in Refs. [13, 24], and we call it clusterization of baryons (CB).

In our CB procedure the diluted nuclear matter is subdivided into many clusters with a coalescence-like recipe. In particular, we assume that baryons (both nucleons and hyperons) can produce a cluster with mass number A if their velocities relative to the center-of-mass velocity of the cluster is less than a critical velocity v_c. Accordingly we require $|\vec{v}_i - \vec{v}_{cm}| < v_c$ for all $i = 1, ..., A$, where $\vec{v}_{cm} = \frac{1}{E_A} \sum_{i=1}^{A} \vec{p}_i$ ($\vec{p}_i$ are momenta and E_A is the summed energy of the baryons in the cluster). In addi-

tion, we assume that the distance between the individual baryons and the center of mass of the clusters should be less than $2 \cdot A^{1/3}$ fm, so these baryons can still interact leading to the nuclei formation. In this case such clusters with nucleons inside have the density of $\rho_c \approx \frac{1}{6}\rho_0$ as it was established in the previous studies of the statistical multifragmentation process [17, 31–37]. Since the baryons do still move with respect to each other inside these clusters, they present an excited nuclear system. The excitation energy of such clusters is calculated according to the method suggested in Refs. [13, 14]. The excitation energy of the clusters is related to the properties of nuclear matter in local equilibrium at the cluster density. It is also connected to the corresponding baryon interaction in matter. These clusters are analogous to the local freeze-out states for the liquid-gas type phase coexistence adopted in statistical models. The following evolution of the clusters, including the formation of nuclei from these baryons, can be described in a statistical way. According to our procedure these hot clusters decay into nuclei. For the description of this process we employ the Statistical Multifragmentation Model (SMM) which describes the production of normal nuclei very well, and it was generalized for the hypernuclear case (see Refs. [17–19, 38, 39]).

Within this approach we have succeeded to describe the yields and energies of light nuclei observed in the FOPI experiment for central collisions of relativistic heavy ions [4, 5], that was not possible with the previous models. It is especially important since we have explained the cross-over behaviour of the ^{3}He and ^{4}He light nuclei production with the beam energy: The ^{4}He yield dominates over ^{3}He at low and intermediate energies, while the ^{3}He yield is larger at high energies. This was previously not understandable within simplistic coalescence models which always produce more light nuclei than heavy ones. The reason of this behaviour is in the decay of the primary large clusters that favor the ^{4}He production in comparison with ^{3}He. For high collision energies the sizes of the primary clusters becomes smaller and leads after their decay to the production of smaller nuclei. The important result of our studies is that the excitation energy of such clusters should not be too high, around ~ 10 MeV per nucleon, i.e., close to the nuclear binding energy. Based on these previous successes of our approach we extend it now to analyze the hypernuclear observations.

III. EXCITED NUCLEAR CLUSTERS AT SUBNUCLEAR DENSITY

In Fig. 1 we show the distributions of protons and Lambda hyperons after the UrQMD simulations of central Au + Au collisions (impact parameters $b \leq 3$ fm) at $\sqrt{s_{NN}}$=3 GeV center-of-mass energy. (The considered Λ do not include Σ^0 hyperons since they decay later than the hypernuclei are formed.) One can see that the
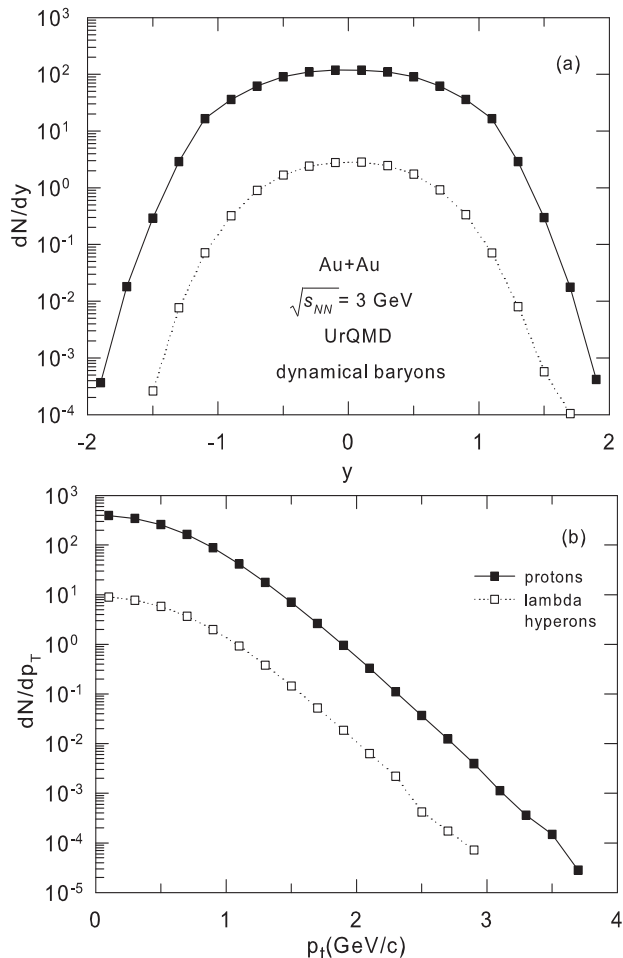
FIG. 1: Total proton and Λ distributions (per event) after UrQMD calculations of central gold collisions at center-of-mass energy of $\sqrt{s_{NN}}$=3 GeV. Top panel (a) - rapidity distributions. Bottom panel (b) - transverse momenta distributions, in the rapidity range $|y| < 0.5$.

baryons have very broad momentum distributions going beyond the projectile and target rapidities. We have also performed the calculations with other models, the Dubna cascade model [13, 23] and the phase space generation of all available particles in the center of mass system [14]. The results are very similar, therefore, we are sure to reproduce the general reaction picture. These distributions characterize the baryon UrQMD input for the following cluster selection. To evaluate the dynamical uncertainties the two time instances, 20 fm/c and 40 fm/c after the collision, are analyzed. Since the interaction rate decreases rapidly the momentum distributions change very little during the times. The coordinate distances between baryons increase towards the later time. Nevertheless, it has a little effect on the following clusterization in the CB procedure in the case when we consider v_c parameters (0.14c and 0.22c) which were previously extracted as the best ones from comparison with FOPI experimental

data [4, 5]. Such a low sensitivity is because the hadron correlations are propagated explicitly in UrQMD.
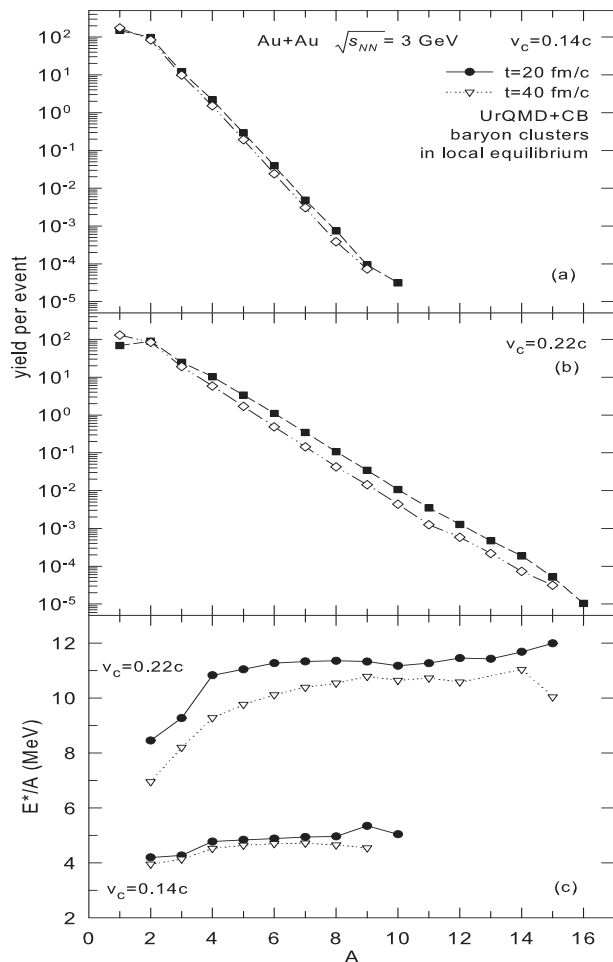

FIG. 2: Calculated distributions of local nuclear clusters (per event) formed from dynamically produced baryons after UrQMD and the clusterization (CB) procedure by using the selection of the baryons with the velocity and coordinate proximity. Top panel (a) - mass distributions of the cluster with the velocity parameter v_c=0.14c. Middle panel (b) - mass distributions of the cluster with the velocity parameter v_c=0.22c. Bottom panel (c) - average excitation energy of the clusters versus their mass number. The times for stopping the UrQMD calculations and v_c parameters are shown in the panels.

The results of the following selection of the baryonic clusters within CB are shown in Fig. 2. We see that the cluster yields decrease nearly exponentially with their masses, and it is similar to a normal coalescence-like process. As was mentioned, in our approach we assume that these clusters are excited nuclear systems in local chemical equilibrium. The bigger clusters can naturally be formed with larger velocities parameters v_c. The time dependence of the cluster sizes is also understandable: It is obvious that the larger coordinate distances between baryons slightly decrease the production of big clusters

because of the larger space separation. The important characteristic is the excitation energy of these clusters, which are presented in the bottom panels. A larger v_c leads to a higher excitation energy, since the relative velocities of the baryons inside the clusters are higher.
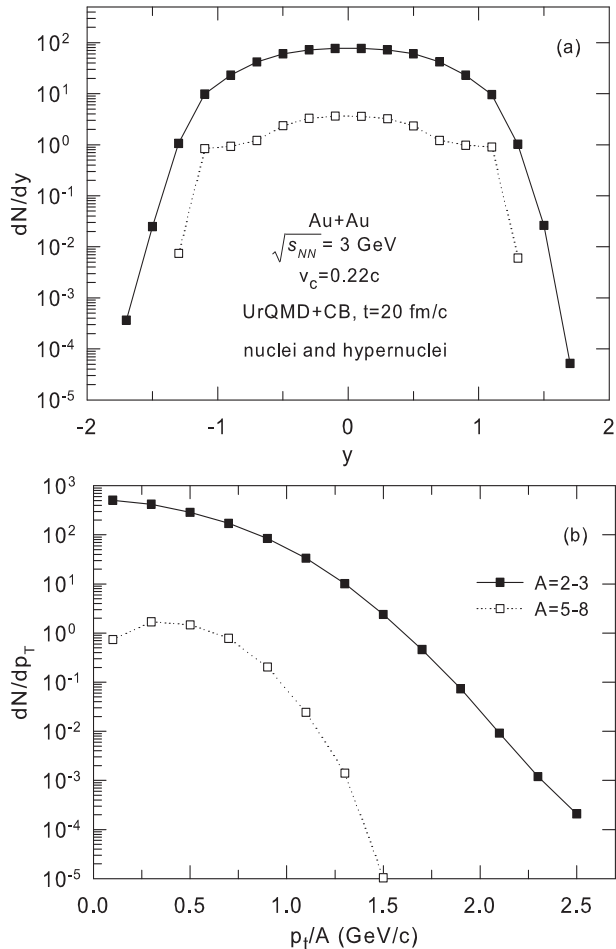
IV. ANALYSIS AND INTERPRETATION OF EXPERIMENTAL DATA

FIG. 3: Rapidity (top panel (a)) and transverse momentum per nucleon (bottom panel (b) overall rapidities) distributions of the excited baryon clusters, which have the mass numbers from A=2 to 3, and from A=5 to 8. Yields are per event.
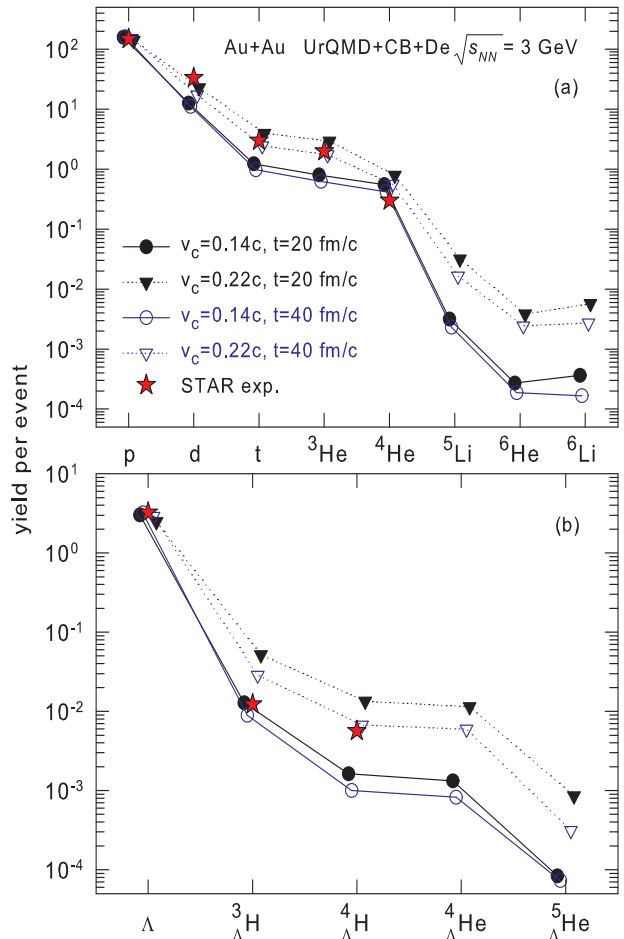

FIG. 4: (Color online.) Comparison of full calculations including UrQMD transport, formation of excited local thermalized clusters (CB) and de-excitation of these clusters (De) with STAR experimental data. The predictions for other important nuclei and hypernuclei are presented too. Top panel (a) - total yields of normal nuclei in central collisions. Bottom panel (b) - total yields of hypernuclei in central collisions. Notations for nuclei, and the used time and v_c parameters are shown in the panels.

The kinematic characteristics of the primary excited clusters (rapidity and transverse momenta) are depicted in Fig. 3, for the case of v_c=0.22c. To evaluate the mass effect we have present two groups of clusters: Small ones, with mass numbers A from 2 to 3, and bigger ones, with mass numbers A from 5 to 8. Reflecting the properties of the initial baryons (Fig. 1) these rapidity and transverse distributions are quite broad. Further information about new nuclei after their production via the decay of such clusters one can find in Refs. [13, 14]. For example, the products of the cluster decay will preserve the kinematic characteristics (per nucleon) corresponding to the dynamically produced baryons. Many new exotic nuclei can be formed, and the specific particle correlations are

the best way to distinguish this reaction mechanism.

In this paper we concentrate only on the analysis of the recent STAR data. The comparison with the experimental data on nuclei and hypernuclei production [9, 40] and the predictions within our approach are shown in Figures 4, 5, and 6. We are able to reproduce the main experimental results (involving the distributions trends) by applying the models discussed in the previous sections with reasonable parameters. Therefore, we believe that the idea including the formation of the baryonic clusters

under local equilibrium and their following statistical disintegration is very promising.

In Fig. 4 we show the yields of some light nuclei and hypernuclei (normalized per event) obtained in central collisions. In the STAR experiment these yields were evaluated with a special procedure, however, we do it on an event per event basis directly from the calculations. We can reach the best description of the data for normal fragments with the mass numbers $A = 2 - 4$ by using the parameter v_c=0.22c . The yields manifest the exponential decreasing with A, that is expected from other experiments too. In our calculations the final nuclei with $A \sim 4$ we have obtained after the de-excitation of local primary clusters with $A \sim 10$ and with the corresponding excitation energy of around 10 MeV per nucleon (see Fig. 2). This excitation energy is consistent with the one extracted from the analyses of other experiments [13, 14].

clei are depicted in Fig. 5. Our calculations are in qualitative agreement with the data. However, the experimental yields of nuclei for larger species show a slight increase towards the target rapidity. We believe it is related to the experimental selection of central events (0–10%) via the particle multiplicity and the applied spectator cut. In reality large multiplicities may be also obtained in quasi-peripheral events, when a large group of nucleons is still located in the target and projectile kinematic regions. These nuclear remnants are excited, and they may even capture hyperons [11, 24]. Namely the decay of such residues can give an additional contribution to the yields of larger nuclei. The goal of the present calculations is to investigate the true central events ($b \leq 3$ fm) without this contribution.
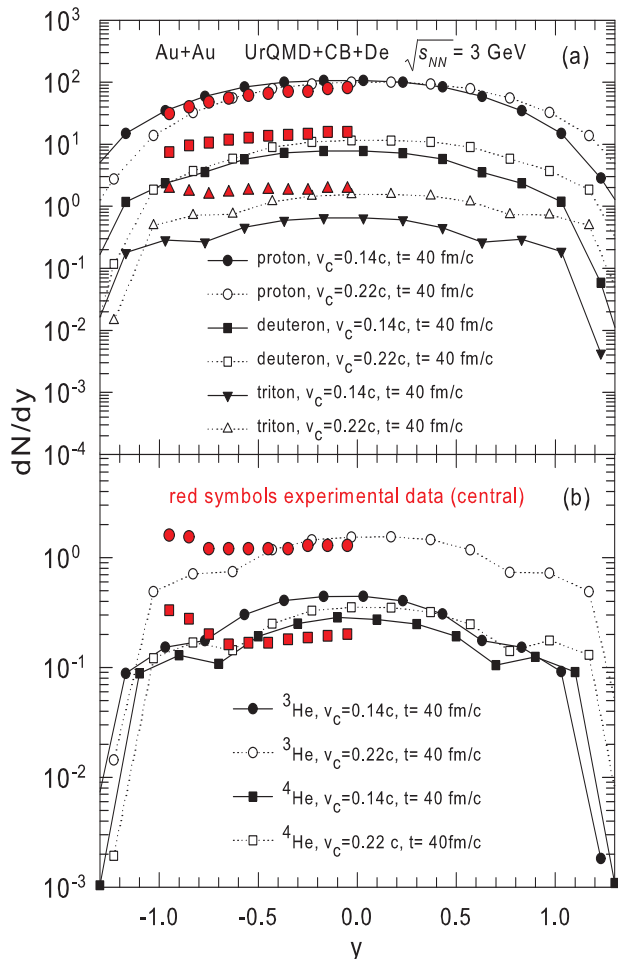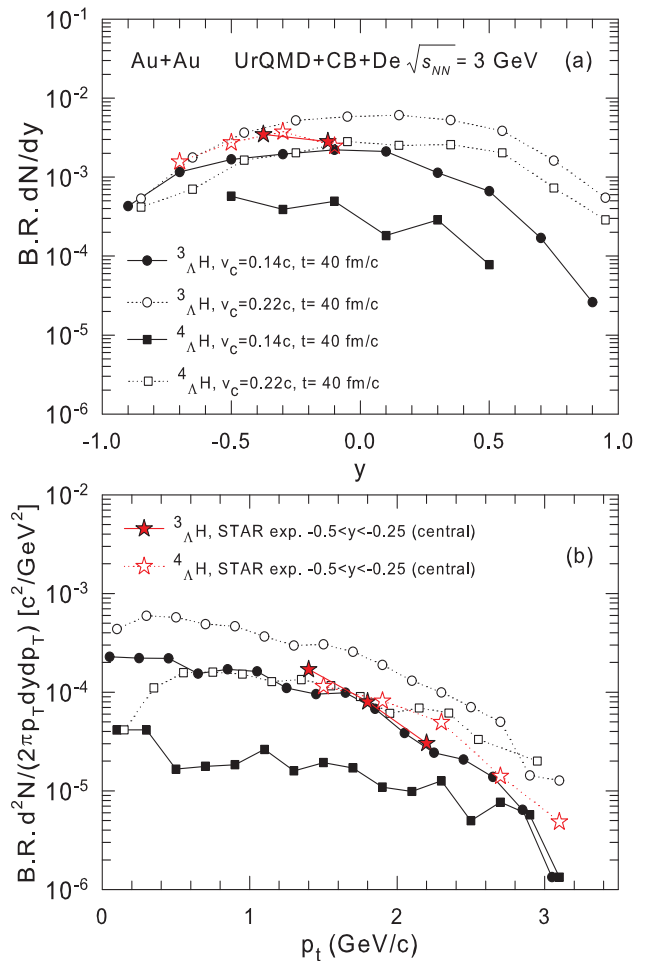

FIG. 5: (Color online.) Comparison of the calculations of the rapidity distributions of normal nuclei produced in central collisions with STAR experimental data [40]. Top panel (a) - protons, deutrons, tritons. Bottom panel (b) - ^{3}He, ^{4}He. The model parameters are indicated in the panels.

The rapidity distributions of produced normal light nu-

FIG. 6: (Color online.) Comparison of the calculations of the rapidity (top panel (a)) and transverse momentum distributions (bottom panel (b)) of $^3_\Lambda$H and $^4_\Lambda$H) hypernuclei with STAR experimental data [9]. The model parameters and the rapidity intervals are shown in the panels. The branching decay ratios (B.R.) are taken into account in the calculations.

Fig. 6 shows the rapidity and transverse momentum distributions of the hypernuclei ($^4_\Lambda$H and $^3_\Lambda$H). We are

able to reproduce correctly the main trends of the distributions. With v_c parameters which are in the range suitable for the description of normal nuclei we may describe the total yield of one of these two hypernuclei. However, we see that in the experiment the production of $^4_\Lambda$H nuclei looks similar to $^3_\Lambda$H nuclei before the branching ratio correction. While in the calculations it is essentially lower, even by taking the corrections into account.

It is also important that by examining carefully Fig. 4 we see an essential difference between the experimental yields of hypernuclei and normal nuclei, which are obtained after all experimental corrections. Namely, the yield ratio of $^3_\Lambda$H to $^4_\Lambda$H is less than a factor 2. Whereas the ratio of ^{3}He to ^{4}He is more than factor 5. To our opinion it is one of the most interesting and puzzling results of this experiment: The general decrease of the yields with mass number A is a quite expected behaviour and it is confirmed by many other experimental measurements. Phenomenologically one can understand it as a low probability to add an additional nucleon to the formed fragments. However, the data seems to suggest that an increase by one neutron for $A = 3$ fragments has a much larger probability in the hypernuclear case as in the case of a normal nucleus.

We think this effect may be used extract an important experimental information on the properties of hypermatter of subnuclear density and on the Λ interaction in this matter. We have investigated possible reasons of this effect within our approach. It is known that the Λ interaction in nuclei is lower than for nucleons approximately by factor $2/3$. One can phenomenologically suppose that it is related to the number of u and d quarks in the baryons. For this reason the excitation energy of the primary local hyper clusters may be lower than in normal clusters. We have performed the corresponding calculations by assuming that the excitation of such clusters are only $2/3$ of the normal clusters to simulate the effects of the hyperon interaction in the low-density clusters. In the same time the properties of normal clusters dominating in the system remain unchanged. We obtain that the yields of $^4_\Lambda$H increases much stronger than $^3_\Lambda$H, and the ratio becomes closer to the experimental one. Another possibility to explain this effect is related to the prolonged space structure of weakly bound $^3_\Lambda$H nucleus formed in the phase transition coexistence region. In the statistical model it can be taken into account by reducing the coordinate phase space of such hypernuclei, as it was suggested before for some normal nuclei [17]. This can decrease the calculated $^3_\Lambda$H yield.

Presently we do not have a sufficient experimental information to distinguish between the two alternative scenarios. In particular, the production of other nuclei and hypernuclei in same reactions is crucially important for the understanding of the underlying physical process. In Fig. 4 we show the predictions for the yields of few heavier nuclei (^{5}Li, ^{6}He, ^{6}Li), and hypernuclei ($^4_\Lambda$He, $^5_\Lambda$He), which should be produced in addition within the corresponding reaction mechanism. The ^{5}Li production can

be measured via its decay into proton and ^{4}He, or into ^{2}H and ^{3}He, with a probability compared with the probability of correlations measured for identification of $^3_\Lambda$H and $^4_\Lambda$H. The $^4_\Lambda$He and $^5_\Lambda$He hypernuclei can be identified via three particle correlations. Generally, more heavy nuclei and hypernuclei are very instructive, because their production is related to fundamental properties of the nucleation in nuclear matter [17, 18, 38, 41]. Therefore, the inclusion of larger nuclei in the analysis will allow to exclude alternative theoretical explanations.

We specifically emphasize the needs for new experiments, and the measurement of new hypernuclei with different masses as extremely important for further progress in hypernuclear physics. The great variety of produced hypernuclei is an important advantage of relativistic heavy ion collisions in comparison with the traditional hypernuclear methods concentrated on reactions leading only to a few species. By comparing the yields of different hypernuclei produced in same reaction one can extract additional information about the properties of hypermatter, and also about exotic hypernuclei [41]. In this respect larger hypernuclear isotopes can provide further information (see also Ref. [42]).

V. CONCLUSIONS

We have applied a novel theoretical approach to explain the yields of light nuclei and hypernuclei measured in the STAR experiment in the central relativistic nuclear collisions. Our approach combines 1) the adequate dynamical models for the baryon production in the first reaction stage, 2) the formation of intermediate local sources in equilibrium (excited large baryonic clusters) at subnuclear density, and 3) the description of the nucleation process inside these sources as their statistical decay. As was shown previously [13, 14] this approach can be successfully used to analyze the production of normal nuclei. We have demonstrated that the present experimental data concerning the production of hypernuclei can also be described within this approach by using similar parameters for the local sources. This may indicate an universal character of the nucleation process in rapidly expanding nuclear matter.

We believe the production of hypernuclei in relativistic ion collisions opens the possibilities to investigate the properties of hypermatter at subnuclear densities, where the nuclei are formed. It is also important in astrophysics for models describing stellar matter in supernova explosions and in binary neutron star mergers. The suggested approach can correctly explain the main trends of the hypernuclear production, and provide consistent quantitative predictions too. We emphasized the puzzle of the relative yields of $^4_\Lambda$H and $^3_\Lambda$H nuclei in comparison with ^{4}He and ^{3}He yields, which can not be explained within the existing models, and which may carry information on the hyperon interaction during the formation of the hypernuclei. This can provide essential complementary

information on the nuclear interaction, and on the nucleosynthesis process at low densities which was previously studied for normal nuclei only. Additional experiments on the comparative yields of several different hypernuclei in same reactions are crucially important.

Acknowledgments

[1] J. Gosset, H. H. Gutbrod, W. G. Meyer, A. M. Poskanzer, A. Sandoval, R. Stock, and G. D. Westfall, Phys. Rev. C **16**, 629 (1977).

[2] W. Neubert and A. S. Botvina, Eur. Phys. J. A **17**, 559 (2003).

[3] W. Neubert and A. S. Botvina, Eur. Phys. J. A **7**, 101 (2000).

[4] W. Reisdorf *et al.*, Nucl. Phys. A **848**, 366 (2010).

[5] W. Reisdorf *et al.*, Nucl. Phys. A **612**, 493 (1997).

[6] A. Andronic, P. Braun-Munziger, J. Stachel, H. Stöcker, Phys. Lett. B **697**, 203 (2011).

[7] B. Dönigus, ALICE collaboration, Nucl. Phys. A **904-905**, 547c-550c (2013).

[8] J.Adam *et al.*, ALICE Collaboration, Phys. Lett. B **754**, 360 (2016).

[9] M. S. Abdallah *et al.*, STAR Collaboration, Phys. Rev. Lett. **128**, 202301 (2022).

[10] R. Abou Yassine *et al.*, HADES Collaboration, EPJ Web of Conferences **271**, 08004 (2022).

[11] A. S. Botvina, K. K. Gudima, J. Steinheimer, M. Bleicher, J. Pochodzalla, Phys. Rev. C **95**, 014902 (2017).

[12] A. S. Botvina, K. K. Gudima, J. Pochodzalla, Phys. Rev. C **88**, 054605 (2013).

[13] A. S. Botvina, N. Buyukcizmeci and M. Bleicher, Phys. Rev. C **103**, 064602 (2021).

[14] A. S. Botvina, N. Buyukcizmeci and M. Bleicher, Phys. Rev. C **106**, 014607 (2022).

[15] J. Aichelin, Phys. Rep. **202**, 233 (1991).

[16] M. Bleicher *et al.*, J. Phys. G **25**, 1859 (1999).

[17] J. P. Bondorf, A. S. Botvina, A. S. Iljinov, I. N. Mishustin and K. Sneppen, Phys. Rep. **257**, 133 (1995).

[18] R. Ogul *et al.*, Phys. Rev. C **83**, 024608 (2011).

[19] R. P. Scharenberg, B. K. Srivastava, S. Albergo, F. Bieser, F. P. Brady, Z. Caccia *et al.*, Phys. Rev. C **64**, 054602 (2001).

[20] A. Le Fevre, J. Aichelin, C. Hartnack, Y. Leifels, Phys. Rev. C **100**, 034904 (2019)

[21] J. Aichelin, E. Bratkovskaya, A. LeFevre,V. Kireyeu,V. Kolesnikov, Y. Leifels, V. Voronyuk, G. Coci, Phys. Rev. C **101**, 044905 (2020)

[22] S. Glässel,V. Kireyeu,V. Voronyuk, J. Aichelin, C. Blume, E. Bratkovskaya, G. Coci, V. Kolesnikov, M. Winn, Phys. Rev. C **105**, 014908 (2022).

[23] V. D. Toneev, K. K. Gudima, Nucl. Phys. A **400**, 173 (1983).

[24] A. S. Botvina *et al.*, Phys. Lett. B **742**, 7 (2015).

[25] A. S. Botvina, J. Steinheimer, M. Bleicher, Phys. Rev. C **96**, 014913 (2017).

[26] S. Sombun, K. Tomuang, A. Limphirat, P. Hillmann, C. Herold, J. Steinheimer, Y. Yan, M. Bleicher, Phys. Rev. C **99**, 014901 (2019).

[27] S.A. Bass *et al.*, Prog. Part. Nucl. Phys. **41**, 255 (1998).

[28] T. Reichert *et al.*, J. Phys. G **49**, 055108 (2022).

[29] T. Reichert, J. Steinheimer, V. Vovchenko, B. Donigus, M. Bleicher, Phys. Rev. C **107**, 014912 (2023).

[30] A. S. Botvina, K. K. Gudima, J. Steinheimer, M. Bleicher, I. N. Mishustin, Phys. Rev. C **84**, 064904 (2011).

[31] B.-A. Li, A. R. DeAngelis and D. H. E. Gross, Phys. Lett. B **303**, 225 (1993).

[32] H. Xi *et al.*, Z. Phys. A **359**, 397 (1997).

[33] M. D'Agostino *et al.*, Phys. Lett. B **371**, 175 (1996).

[34] N. Bellaize *et al.*, Nucl. Phys. A **709**, 367 (2002).

[35] J. Iglio *et al.*, Phys. Rev. C **74**, 024605 (2006).

[36] V. E. Viola *et al.*, Nucl. Phys. A **681**, 267c (2001).

[37] V. A. Karnaukhov *et al.*, Phys. At. Nucl. **69**, 1142 (2006).

[38] A. S. Botvina and J. Pochodzalla, Phys. Rev. C **76**, 024909 (2007).

[39] A. S. Lorente, A. S. Botvina, and J. Pochodzalla, Phys. Lett. B **697**, 222 (2011).

[40] Hui Liu for STAR Collaboration, Acta Phys. Polon. B, Proc. Suppl. **16**, 1–A148 (2023).

[41] N. Buyukcizmeci, A. S. Botvina, A. Ergun, R. Ogul, M. Bleicher, Phys. Rev. C **98**, 064603 (2018).

[42] A. Kittiratpattana *et al.*, arXiv.org/abs/2305.09208 [nucl-th], 2023.